

## Environmental Factors Affecting Corrosion of Steel Inserts in Ancient Masonry

**Luca Bertolini**<sup>1</sup>

**Maddalena Carsana**<sup>2</sup>

**Bruno Daniotti**<sup>3</sup>

**Eleonora Marra**<sup>4</sup>

### ABSTRACT

Steel inserts are often present in ancient masonry in order to improve the structural behaviour of buildings or to prevent the propagation of cracks. Though, the presence of inserts embedded in the materials of the masonry (e.g. mortar, bricks) may be harmful for the durability of the whole structure, since their corrosion may produce deleterious expansive phenomena leading to cracking and detachment of the covering materials. Inserts may have a complex corrosion behaviour, which depends on the material they are in contact and its moisture content. Starting from this problem, the paper shows the preliminary results of a study on the corrosion behaviour of steel inserts embedded in masonry. The effect of temperature and moisture on corrosion rate of steel and resistivity of mortar and brick specimens exposed in a climatic chamber to cycles of temperature (20-40°C) and relative humidity (65-80-95%) are discussed. In order to extend the results obtained on small-scale specimens to case studies that should consider the effect of the real hygrothermal conditions on corrosion of steel inserts in ancient masonry, numerical simulations have been also performed. The results obtained have shown that corrosion rate is negligible in specimens exposed to 65-80% RH (even at 40°C), whereas it has reached high values in wet environments or in the presence of water suction. A correlation between electrical resistivity of embedding materials and corrosion rate of steel has been observed. The validation of these data by means of a bi-dimensional HMT model is now in progress.

### KEYWORDS

Corrosion, steel inserts, ancient brick masonry, hygrothermal conditions, electrical resistivity

---

<sup>1</sup> Politecnico di Milano, CMIC Dep, Milano, ITALY, [luca.bertolini@polimi.it](mailto:luca.bertolini@polimi.it)

<sup>2</sup> Politecnico di Milano, CMIC Dep, Milano, ITALY, [maddalena.carsana@polimi.it](mailto:maddalena.carsana@polimi.it)

<sup>3</sup> Politecnico di Milano, BEST Dep, Milano, ITALY, [bruno.daniotti@polimi.it](mailto:bruno.daniotti@polimi.it)

<sup>4</sup> Politecnico di Milano, BEST/CMIC Dep, Milano, ITALY, [eleonora.marra@chem.polimi.it](mailto:eleonora.marra@chem.polimi.it)

## 1 INTRODUCTION

Steel inserts are often present in ancient masonry, either due to an original design choice or as the result of later restoration works. They may have different aims, e.g. improving the structural behaviour of buildings (chains and ties) or preventing the propagation of cracks, and they may be applied externally or embedded in the materials of the masonry (mortar, bricks, stone blocks, etc.). In the latter case, the presence of these elements may be harmful for the durability of ancient masonry, since their corrosion may produce deleterious expansive phenomena leading to the detachment of the covering materials [Bertolini *et al.* 2009, Lourenco 2006, Straube & Schumacher 2006].

It is important to make a distinction between steel inserts dated to the creation of the original structure, normally embedded in the structural elements, and those fixed later during restoration phases (most often applied externally). While externally applied steel inserts are directly exposed to the action of the atmosphere (either inside or outside the building), inserts embedded in the masonry may have a complex corrosion behaviour, which depends on the material they are in contact (e.g. bricks, hydraulic mortars, gypsum) and its moisture content. Microstructure of these materials and chemical composition of the solution contained in their pores will influence the corrosion behaviour of steel. For example, the nearly neutral pH of some types of mortar can cause the corrosion process on the steel surface as soon as they are wet; conversely, in the case of alkaline mortars that promote passivity of the steel, corrosion can only take place after carbonation of the mortar cover has occurred. The corrosion rate will also depend on the availability of water and oxygen in the pores of the embedding material near the steel surface, hence it will be a function of environmental conditions. Temperature and humidity of the environment influence the electrical resistivity of the mortar or bricks and the corrosion rate of the embedded steel insert. As instance, a mortar with very high moisture content (that is near saturation, e.g. due to wetting or water condensation) is characterized by low resistivity, but, if saturation conditions are maintained for long time, the oxygen content at the steel surface may be low due to the low diffusivity through the water-filled pores. Conversely, in the case of masonry characterized by lower water content, although oxygen is available at the steel surface, the resistivity is high and it increases as the moisture content decreases.

Concerning masonries, rarely condition of permanent saturation are reached, thus oxygen is available at the steel surface and the corrosion rate depends on the resistivity of the materials in contact with steel; in general, the lower the moisture content, the higher the electrical resistivity of these materials and the lower the corrosion rate of steel. Nevertheless, a large number of parameters, related to both the environment and the materials, may have a complex role, which makes any prediction of the actual corrosion behaviour of steel inserts quite difficult. As matter of facts, the study of the dependence of resistivity of masonry and corrosion rate of steel insert on the environmental conditions is a subject of great interest in relation to optimising restoration methods and promoting a durability approach for historical buildings. Improving the understanding on corrosion of steel embedded in masonry could provide a tool for the design, of repair works which are not merely aimed at the remediation of corrosion damages, but also at the control of the corrosion rate necessary to fulfil conservation requirements of preserving as much as possible the original materials.

This paper shows the preliminary results of a study on the corrosion behaviour of steel inserts embedded in brick masonry. The first part of this study deals with the assessment of the corrosion behaviour of low carbon steel embedded in mortar, brick and composite brick and mortar samples, exposed to several environments. The effect of temperature and humidity on corrosion rate of steel and resistivity of specimens exposed in a climatic chamber to cycles of temperature (20-40°C) and relative humidity (65-80-95%) are discussed. In order to extend the results obtained on small-scale specimens to case studies that should consider the effect of the real hygrothermal conditions on corrosion of steel inserts in ancient brick masonry, numerical simulations have been performed. Although different types of mortars (based on several types of binders: gypsum, lime, or blends of gypsum-lime, lime-pozzolana and lime-cocciopesto) have been considered in the study; only

preliminary results concerning fired brick and a mortar based on gypsum-lime blend will be considered in this paper.

## 2 CORROSION OF LOW CARBON STEEL EMBEDDED IN BUILDING MATERIALS

### 2.1 Experimental procedure

#### 2.1.1 Materials and specimens description

In order to study the behaviour of steel embedded in a masonry made of fired bricks and a blended lime-gypsum mortar, different sets of specimens have been manufactured: mortar specimens (LG), composite brick and mortar specimens (B+LG) and, finally, brick specimens (B). In  $80 \times 90 \times 30 \text{ mm}^3$  lime-gypsum mortar samples, two carbon steel bars (6 mm in diameter) and two stainless steel wires (AISI 304, 2 mm in diameter) have been inserted. Brick specimens have a size of  $55 \times 120 \times 60 \text{ mm}^3$ , in order to obtain many samples from the same brick; in two of these specimens two carbon steel bars (6 mm in diameter) have been inserted in two holes and the space between the bar and the brick has been filled with lime-gypsum mortar; in the other specimen bars have been forced in direct contact with the brick. A sketch of specimen geometry is shown in Fig. 1. The blended lime-gypsum mortar has been prepared using the following mix proportions ( $\text{kg/m}^3$ ): lime 212, gypsum 430, sand 769 and water 404, resulting in a 0.63 water/binder ratio and a 30% flow measured on the flow table ( $D_m = 130 \text{ mm}$ ). Concerning brick samples, reused fired masonry bricks have been used. Finally, as far as steel bars are concerned, a low carbon steel (C 0.04%, Si 0.041%, Mn 0.285%, S 0.012% and P 0.012%) and ferritic microstructure (grains size of about  $20 \mu\text{m}$ ) and little pearlitic inclusions, has been used.

#### 2.1.2 Environmental conditions

Mortar specimens have been cast in PVC moulds and demoulded after 5 days, following the procedure described in the EN 1015-11 standard. Every sample has been cured for 28 days in a climatic chamber (7 day at 95% RH and 21 days at 65% RH,  $20^\circ\text{C}$  T). At the end of the curing time all the specimens have been kept in a carbonation chamber (0.2%  $\text{CO}_2$ , 65% RH and  $20^\circ\text{C}$ ), until complete carbonation has been achieved (14 and 28 days respectively for the composite brick and mortar and for the mortar specimens), as shown by tests with an alcoholic solution of phenolphthalein. At the end of curing, specimens have been exposed to several environments.

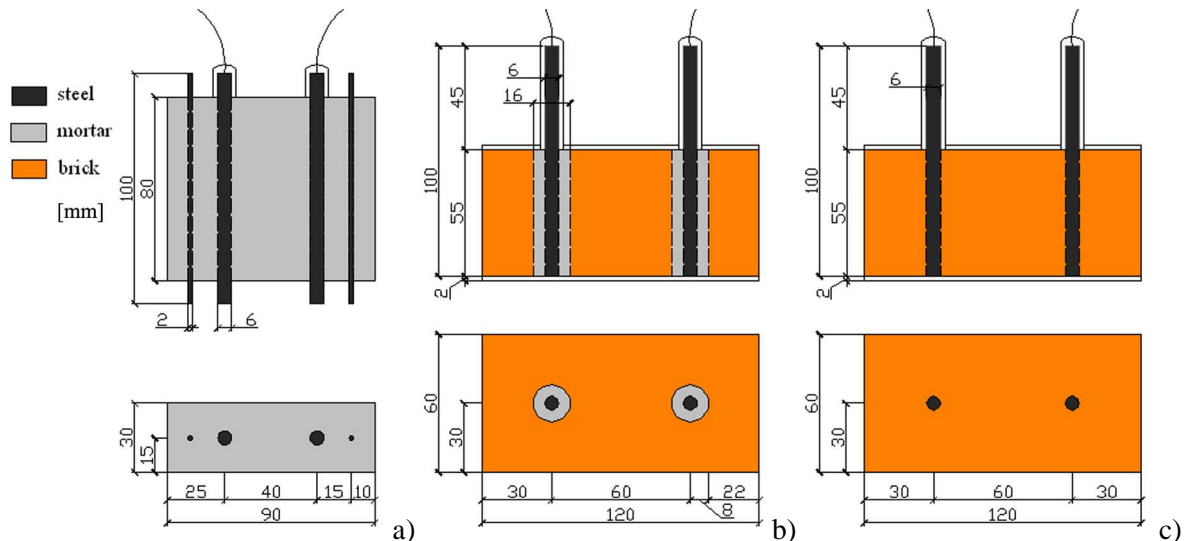


**Figure 1.** Longitudinal section (up) and cross-section (low) of the specimens manufactured in the laboratory: a) blended lime-gypsum mortar sample (LG) with 2 low carbon steel bars and 2 stainless steel wires; b) composite brick and mortar sample (B+LG) with 2 low carbon steel bars embedded in a 5 mm mortar layer; c) fired brick sample (B) with 2 low carbon steel bars. Dimensions in mm.

Brick and composite brick and mortar specimens have been exposed to three moisture conditions, keeping constant the temperature at 20°C: 95% RH (C1), water (C2), and again 95% RH (C3). In the case C2, only 10 mm of the samples has been put in water, to allow water uptake towards steel bars placed at 20 and 60 mm from the water surface. As far as mortar specimens are concerned, instead, they have been exposed to six different environments, varying relative humidity (65-80-95%) and temperature (20-40°C). Each condition has been kept for at least 28 days, apart from the storage in water (7 days). Finally, one of the three mortar samples has been further exposed to the moisture conditions (C1, C2 and C3) undertaken by the brick-based specimens (though, storage in C2 has been kept only for 1 day, maintaining steel bars at 20 and 80 mm from the water surface).

### 2.1.3 Corrosion measurements

Corrosion behaviour of specimens has been investigated by monitoring electrical resistivity of the mortar or brick ( $\rho$ ,  $\Omega\text{m}$ ), corrosion potential ( $E_{\text{corr}}$ , mV vs Ag/AgCl) and corrosion rate ( $i_{\text{corr}}$ ,  $\text{mA}/\text{m}^2$ ) on the steel bars. Resistivity measurements could provide information about the moisture content of specimens and their porosity. Electrical conductance ( $G$ , mS) has been measured with a conductivitymeter and converted in resistivity by using the relationship:  $\rho = K / G$  (where  $K$  is the cell constant that considers the specimen geometry, which was determined with a FEM model); these measurements have been carried out using pairs of stainless steel wires (in the case of LG samples) or carbon steel bars (in the case of B and B+LG specimens), linked to the conductivitymeter. Corrosion potential has been measured versus an external reference electrode (Ag/AgCl) using a high impedance voltmeter. Finally, corrosion rate has been measured with the polarisation resistance  $R_p$  method, by imposing potential steps of  $\Delta E = \pm 10$  mV versus the corrosion potential and measuring the resulting current density ( $i$ ,  $\text{mA}/\text{m}^2$ ); corrosion rate has been calculated as:  $i_{\text{corr}} = B / (\Delta E/i)$ , considering  $B = 26$  mV [Bertolini *et al.*, 2004]. With regard to the measurement of corrosion rate on LG samples, stainless steel wires have been used as counter electrodes; carbon steel bars have been utilized in turn as counter electrode or working electrode in the case of B and B+LG specimens.

## 2.2 Results and discussion

Figure 2a shows corrosion potential (empty symbols) and corrosion rate (filled symbols), as a function of time, of different specimens (LG, B and B+LG) in three different moisture conditions (at 20°C): humid environment at 95% RH (C1), wet (C2), and again humid (C3). Red, green and blue curves represent an average of the measurements performed respectively on different replicate bars. Corrosion potential values corresponding to -200 mV vs Ag/AgCl (suggesting negligible corrosion) have been registered only on brick-based specimens (B and B+LG) in the 95% RH condition (C1), while in all the other cases corrosion potential falls to -400÷-600 mV showing active corrosion. These observations are supported by the corrosion rate measurements: indeed, only in brick-based samples (B and B+LG) in humid condition (C1) negligible corrosion rate have been measured (being the threshold conventionally fixed at  $1 \text{ mA}/\text{m}^2$ , which is equal to  $1.17 \mu\text{m}/\text{year}$ , assuming uniform corrosion); in the other situations, moderate ( $2 \text{ mA}/\text{m}^2$  on LG sample, in environment C1) or even high ( $10\div 100 \text{ mA}/\text{m}^2$  on every other sample, in C2) corrosion rates have been observed. Table 1 shows the average values and standard deviations of steady state measurements in each exposure condition (C3 condition has been excluded since steady values have been not reached). In this table, for condition C2, separate values are reported for corrosion potential and corrosion rate of bars at different distance from the water uptake surface (20 and 60÷80 mm). Lower bars, at 20 mm that experienced a higher water content have shown higher corrosion rate, though, LG specimen was more affected by this phenomenon.

Corrosion behaviour of steel can be correlated to results of electrical resistivity measurements. Indeed, Fig. 2b shows the resistivity, as a function of time, of the specimens. Extremely high values of resistivity have been achieved in C1 condition by B+LG specimens (red curve represents an average of two replicate specimens). This could be attributed to the presence of a discontinuity between the brick and the mortar layer; though, further investigations are required for a full comprehension of such an aspect. Lower resistivity is shown by LG (blue curve, about  $1100 \Omega\text{m}$ ) and especially B

(green curve, about 500  $\Omega\text{m}$ ) specimens, the latter being more porous than the former. In wet condition (C2) these differences tend to become negligible (values roughly 10÷40  $\Omega\text{m}$ ), whereas in the final condition (C3) there is a progressive recover of the initial differences. Comparing the wetting process with the drying one, it is possible to notice the differences in the kinetic of the hygrometric pattern: in the former case (C1-C2 boundary) the transient is very short (constant curve is reached in few hours), while in the latter (C2-C3 boundary) is slower (resistivity returns to its first range value in more than 10 days). Moreover, the drying process seems to be quicker in the B+LG specimens, followed by the B sample and by the LG one.

Since electrical resistivity measurements can provide information about the water content of specimens and their porosity, it could be used as a corrosivity index in the different environments. In general, the lower the resistivity of the embedding material, the higher the corrosion rate of inserts. This can be clearly observed in Fig. 3a, where the relationship between electrical resistivity and corrosion rate in the specimens is presented, hence allowing an evaluation of the influence of different hygrothermal conditions on such parameters. As a matter of fact, in the B+LG samples (red curve) the safest condition has been achieved (highest resistivity and lowest corrosion rate), if compared to that reached in the B specimen (green curve) and in the LG one (blue curve).

Also in the case of the LG mortar specimens, it could be useful to analyse the relationship between electrical resistivity and corrosion rate (Fig. 3b). Each of them has been stored at a fixed relative humidity, just varying the temperature (blue curve refers to 20°C and red one to 40°C). As far as corrosion rate is concerned, it is below 1 mA/m<sup>2</sup> for samples stored at both 65% RH (empty symbols) and 80% RH (filled symbols), whatever the temperature is. At 95% RH (bold symbols), instead, corrosion rate increases up to 10 mA/m<sup>2</sup>. With regards to electrical resistivity values, they decrease as the moisture level increases; this happens at any temperature, even though this is more evident at 40°C. Concerning the role of temperature, it can be also observed that in dry environment (65% RH) an increase in temperature enhances drying out hence reducing the corrosion rate of bars (below 0.01 mA/m<sup>2</sup>); as relative humidity raises (80% RH), this effect is reduced to the point of being negligible. Indeed, at 95% RH the increase in the kinetic of the corrosion process is the key factor, so corrosion rate is higher at 40°C (10 mA/m<sup>2</sup>) than at 20°C (3 mA/m<sup>2</sup>). In Table 2, average values and standard deviation of resistivity, corrosion rate and corrosion potential values, measured on LG mortar, are reported.

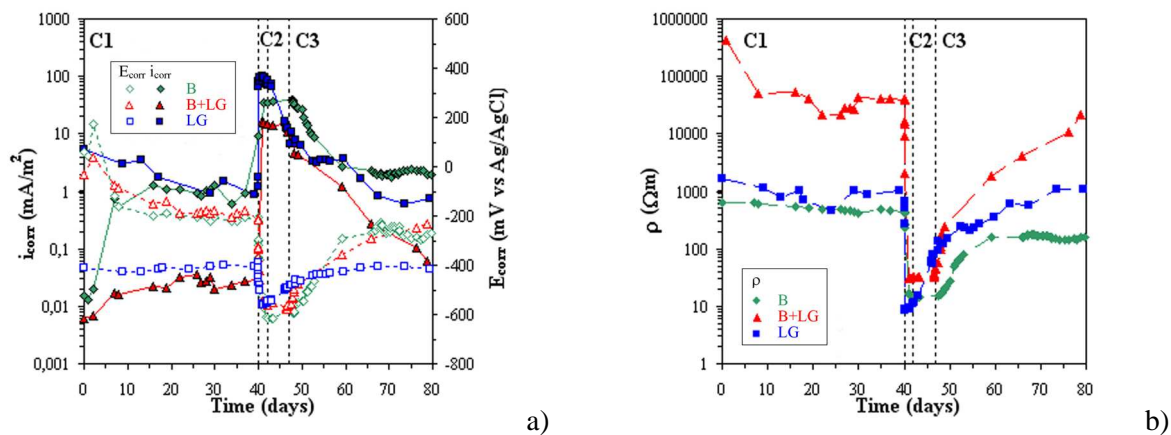


**Figure 2.** a) Corrosion potential  $E_{\text{corr}}$  and corrosion rate  $i_{\text{corr}}$ , as a function of time, of steel bars embedded in different materials, in three exposure conditions at 20°C (C1 and C3 refer to 95% RH, while C2 refers to wet environment). Green, red and blue symbols refer respectively to brick (B), composite mortar and brick (B+LG), mortar samples (LG); empty symbols refer to  $E_{\text{corr}}$  values, filled ones to  $i_{\text{corr}}$  values. b) Electrical resistivity  $\rho$ , as a function of time (same specimens and exposure conditions). Average values of replicate specimens (4 bars for LG, and 2 bars for B and B+LG).

**Table 1.** Mean value  $\mu$  and standard deviation  $\sigma$  of electrical resistivity  $\rho$ , corrosion potential  $E_{corr}$  and corrosion rate  $i_{corr}$  measured on brick (B), brick and blended lime-gypsum mortar (B+LG), blended lime-gypsum mortar (LG), exposed to different environmental conditions.

Environmental condition	Material	$\rho$ [ $\Omega m$ ]		$E_{corr}$ [mV vs Ag/AgCl]		$i_{corr}$ [mA/m <sup>2</sup> ]	
		$\mu$	$\sigma$	$\mu$	$\sigma$	$\mu$	$\sigma$
T 20°C RH 95% (C1)	B+LG	36532	14001	-197	77	0.03	0.01
	B	482	51	-201	32	0.97	0.22
	LG	1072	535	-415	10	2.06	1.65
T 20°C in H <sub>2</sub> O (C2)	B+LG	39	2	-510 (a)	76 (a)	3.53 (a)	0.55 (a)
				-587 (b)	9 (b)	9.95 (b)	1.15 (b)
				-579 (b)	55 (b)	35.25 (b)	5.01 (b)
	B	16	3	-545 (a)	20 (a)	33.72 (a)	1.65 (a)
				-579 (b)	55 (b)	35.25 (b)	5.01 (b)
				-472 (a)	54 (a)	64.93 (a)	9.84 (a)
LG	9	0	-494 (b)	60 (b)	118.93 (b)	16.65 (b)	

(a) bars at 60÷80 mm, (b) bars at 20 mm from the water uptake surface

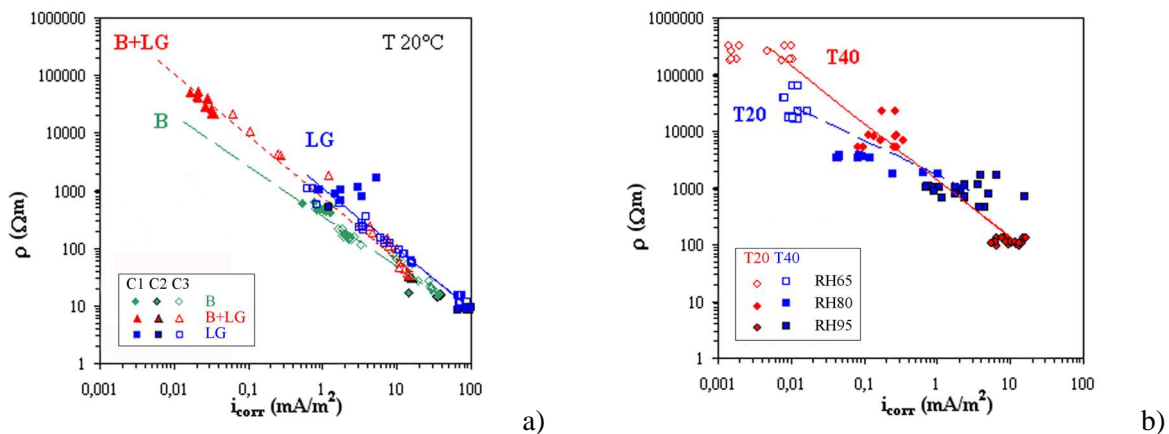


**Figure 3.** a) Relationship between electrical resistivity  $\rho$  and corrosion rate  $i_{corr}$  in different materials during the exposure to various RH conditions (T constant at 20°C). Green, red and blue symbols refer respectively to brick (B), composite mortar and brick (B+LG), mortar samples (LG). Filled symbols refer to 95% RH (C1), bold ones to water uptake (C2), empty ones to drying at 95% RH (C3). b) Relationship between electrical resistivity  $\rho$  and corrosion rate  $i_{corr}$  in blended lime-gypsum mortar samples (LG) during the exposure to different hygrothermal conditions. Red and blue symbols refer to 40°C and to 20°C; empty symbols refer to 65% RH, filled ones to 80% RH, bold ones to 95% RH.

**Table 2.** Mean value  $\mu$  and standard deviation  $\sigma$  of electrical resistivity  $\rho$ , corrosion potential  $E_{corr}$  and corrosion rate  $i_{corr}$  measured on blended lime-gypsum mortar (LG), exposed to different environmental conditions.

Environmental condition	$\rho$ [ $\Omega m$ ]		$E_{corr}$ [mV vs Ag/AgCl]		$i_{corr}$ [mA/m <sup>2</sup> ]		
	$\mu$	$\sigma$	$\mu$	$\sigma$	$\mu$	$\sigma$	
T 20°C	RH 65%	28096	10339	-241	28	0.01	<0.00
	RH 80%	2567	1685	-360	39	0.39	0.36
	RH 95%	935	475	-415	10	3.17	2.59
T 40°C	RH 65%	239199	155042	-219	34	0.01	<0.01
	RH 80%	9235	10683	-413	23	0.21	0.12
	RH 95%	113	44	-359	25	10.24	3.25

### **3 HYGROTHERMAL SIMULATIONS**

Laboratory trials have highlighted the key role of temperature, relative humidity and water (rising damp, condensation or rainwater) on the corrosion behaviour of steel bars embedded in masonry materials. Though moisture and temperature conditions within a brick masonry wall consist of a complex set of parameters (e.g. material properties, indoor and outdoor environmental conditions), taking into account for all these variables could be done by means of hygrothermal models. Indeed, heat and moisture transfer (HMT) models and tools have had a great spread in the last two decades [Straube, J & Burnett, E.F.P. 2001], and have shown a good aptitude in predicting moisture and temperature conditions with a reasonable degree of accuracy [Künzel 1995]. Therefore, in order to extend the results obtained in the laboratory on small-scale specimens, numerical simulations have been performed: temperature, relative humidity and water conditions at the interface between the metal inserts and the materials in which they are embedded have to be analysed. By now, an effort to do the first steps in the definition of the kind of analysis requested (steady or unsteady state) and in the selection of the input data (defining geometry, material characteristics and environmental conditions) for the hygrothermal simulations have been done. Moreover, a preliminary assessment of thermal and hygrometric behaviour of brick masonries exposed to Milan climate and to several laboratory climatic chambers conditions has been performed.

#### **3.1 Simulation models**

As far as preliminary assessment is concerned, two series of simulations have been performed, both considering mono-dimensional geometries and implementing a finite difference algorithm: the first one studies only the temperature field; the second one analyses the simultaneous effects of temperature and relative humidity. In particular, concerning temperature and relative humidity variations, the behaviour of a typical ancient brickworks (consisting of non-hydraulic mortar and fired bricks, width 380 mm) has been studied by means of different hygrothermal boundary conditions, which are steady state ones (20°C T, 50% RH) and dynamic sinusoidal ones (48, 24, 12, 6 and 3 hours periods, mean value and maximum variation respectively of 20°C and 5°C for T, 50 and 15% for RH). Moreover, two further series of situations have been modelled. The first one simulates again traditional brick masonries (width 380 mm), assuming as external boundary condition a reference year in the geographic area of Milan, whereas as internal boundary condition constant temperature and relative humidity (20°C T, 50% and 65% RH) has been considered. In order to validate the experimental data obtained in the laboratory, instead, the second one reproduces brick blocks (width 120 mm) subject to the hygrothermal fluctuations laboratory tests conditions: temperature steps have been imposed (20-40°C), keeping constant the relative humidity (65-80-95%); in addition, relative humidity steps have been fixed (65-80-95%), keeping constant the temperature (20-40°C).

#### **3.2 Results and discussion**

The simulations results have shown that an unsteady state analysis is needed for a consistent evaluation of the thermal behaviour of the brick masonries considered (Fig. 4a), whereas a steady state approach is enough to describe the hygrometric behaviour inside the domain, apart from the boundary zone (Fig. 4b): while the thermal fluctuations involve the whole samples thickness, the relative humidity variations are limited to the very first centimetres from the interface with the environment. The simulations of the experimental laboratory tests, confirming such results, have highlighted a very fast thermal response (24 hours are enough to reach the equilibrium with the environment) and a slower hygrometric one (asymptotic values are not reached in the core region). Finally, since these results have to be validated by the experimental laboratory data concerning the corrosion behaviour of steel inserts, an attempt to consider bi-dimensional HMT models is in progress.

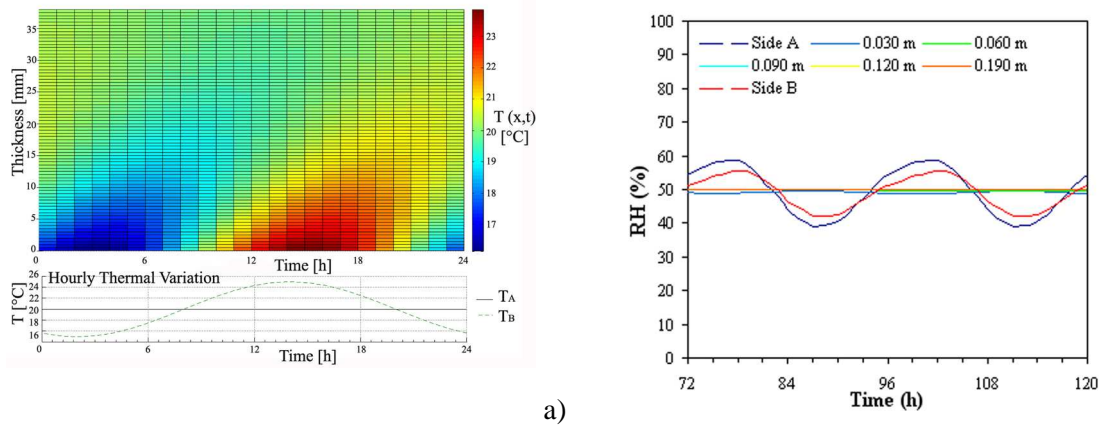


**Figure 4.** a) Thermal response of a 380 mm brick masonry wall to a sinusoidal variation, 24 hours period on side A (down), constant on side B (up). b) Hygrometric response of the same wall to a sinusoidal variation, 24 hours period on side A (blue curve), constant on side B (red curve).

## 4 CONCLUSIONS

This study has shown the key role of temperature, relative humidity and water on the corrosion behaviour of low carbon steel inserts embedded in masonry materials. Tests in specimens with blended lime-gypsum mortar and fired brick have shown that corrosion rate is strongly related to the moisture content of the embedding material. Corrosion rate was negligible in specimens exposed to relative humidity of 80% and 65%, even at 40°C. Conversely, in wet environments or in presence of water suction, corrosion rate has reached high values. A clear correlation between electrical resistivity of embedding material and corrosion rate of steel has been observed. Moreover, with the aim to extend the results obtained on small-scale laboratory specimens to case studies that should consider the effect of the real hygrothermal conditions on corrosion of steel inserts in ancient brick masonry, numerical simulations have been performed. Concerning this, an attempt to define a bi-dimensional HMT model, which can predict corrosion behaviour of inserts as a function of the hygrothermal conditions, is now in progress.

## REFERENCES

- Bertolini, L., Carsana, M. & Marra, E. 2009, 'Degradation of mortars and steel inserts from the ciborium of the medieval abbey of San Pietro al Monte', in *Special Topics on Materials Science and Technology – An Italian Panorama*, Brill Publisher.
- Bertolini, L., Elsener, B., Pedferri, P. & Polder, R. 2004, *Corrosion of steel in concrete*, Wiley-VCH.
- Künzel, H.M. 1995, *Simultaneous Heat and Moisture Transfer in Building Components*, IBP Verlag.
- Lourenco, P.B. 2006, 'Recommendations for restoration of ancient buildings and the survival of a masonry chimney', *Construction & Building Materials*, 20, 239–251.
- Straube, J. & Burnett, E.F.P. 2001, 'Overview of hygrothermal (HAM) analysis methods', in *ASTM Manual Series MNL 40 – Moisture analysis and condensation control in building envelopes*, ed. H.R. Trechsel, Philadelphia, pp. 81–89.
- Straube, J. & Schumacher C. 2006, 'Assessing the durability impacts of energy efficient enclosure upgrades using hygrothermal modelling', *WTA-Journal*, 2, 197–222.